MECHANICAL PERFORMANCE AND PLASTIC SHRINKAGE CHARACTERISTICS OF CONCRETES REINFORCED WITH BASALT FIBRES

John Branston[1,2], Emad Booya[1,3], Karla Gorospe[1,4], and Sreekanta Das[1,5]

[1] University of Windsor, Canada

[2] branstoj@uwindsor.ca

[3] booya@uwindsor.ca

[4] gorospek@uwindsor.ca

[5] sdas@uwindsor.ca

Abstract: In recent years, there has been an increase in the use of sustainable fibres to reinforce concrete composites. Basalt fibres, in particular, have gained popularity in the concrete industry due to its excellent mechanical properties and environmentally-friendly manufacturing process. Typically, the tensile strength of basalt fibres is marginally higher than E-glass fibres and significantly higher than steel fibres. In this two-phase study, the properties of various types of basalt fibres were investigated. In phase I, the compressive, flexural, and impact strength of basalt fibre reinforced concretes were evaluated. The performance of bundle dispersion basalt fibres, basalt minibars, and commonly used steel fibres were compared. In phase II, the effect of filament dispersion fibres on free plastic shrinkage of reinforced concrete overlays was examined. Results from this study showed that the addition of filament dispersion fibres were effective in controlling shrinkage strains.

1   INTRODUCTION

Unreinforced concrete (plain concrete) is susceptible to cracking when it is subjected to tensile stresses. The addition of dispersed fibres into the concrete mixture can bridge and prevent the growth of cracks. This mechanism thereby improves the mechanical characteristics and behaviour of plain concrete. The use of basalt fibres as concrete reinforcement has gained popularity in recent years because of its excellent mechanical properties. In addition, basalt fibers are cheaper and more sustainable compared to conventional fibres. Hence, various types of basalt fibre reinforcing materials have since been developed. These types of basalt fibres include bundle dispersion fibres, filament dispersion fibres, and minibars. It has been found that the tensile strength of basalt fibres is slightly higher than E-glass fibres and considerably higher than steel fibres. Moreover, the manufacturing process of basalt fibres is considered environmentally-friendly (Branston et al. 2016a).

Recent studies into basalt fibres mainly focused on essential mechanical properties such as compressive, flexural, and split-tensile strength. These studies reported that the addition of bundled basalt fibres was beneficial when 0.3% to 0.5% by volume of fibre is added to the concrete mixture (Borhan et al. 2013, Iyer et al. 2015, Jiang et al. 2014). According to Dias et al. (2005) and Ayub et al. (2005), the optimum fibre content differs significantly in various concrete types (i.e., geopolymer and high strength concretes). Moreover, results showed that reinforcing concretes with up to 4% by volume of basalt minibars greatly improves the overall mechanical properties of the concrete (Adhikari et al. 2013). Nonetheless, studies

have shown that the addition of bundled fibres and minibars does not improve compressive strength (Borhan et al. 2013). However, Iyer et al. (2015) reported that the use of basalt filament dispersion fibres increased the compressive strength to up to 31%. Other studies suggest that the use of bundled fibres and minibars shifts the concrete failure mode from brittle to a more ductile one (Jiang et al. 2014, Ayub et al. 2014).

One of the well-known drawbacks of concrete material is its tendency to shrink, resulting in cracks when it is restrained. This problem is more evident in large concrete structures such as pavements, slabs, overlays, and walls. Plastic shrinkage is the volumetric contraction of cement-based materials. It develops at an early age when the concrete is still in its plastic state. At this stage, the concrete does not have the strength to carry any considerable load. The plastic shrinkage of concrete is caused by autogenous mechanisms and capillary stresses in the near-surface pores (Branston et al. 2016a). When water in the cement paste evaporates due to high temperature exposures, negative capillary pressure is developed, which reduces the volume of the cement paste. The rise in capillary pressure, to a critical limit, inside the pores causes the development of disconnected spots with voids in between (Soroushian and Ravanbakhsh 1998).

Researchers have found many ways to control plastic shrinkage. One popular solution is the utilisation of fibres. In general, reinforcing cement composites with fibres mitigates shrinkage cracking, reduces crack widths, reduces overall strains, and minimizes autogenous shrinkage. Furthermore, fibres are capable of bridging cracks, thereby enhancing durability (Banthia and Gupta 2007). Adding fibres with diameters smaller than 40 microns and with aspect ratios of more than 200 have been found to effectively eliminate plastic shrinkage cracking in concrete (Naaman et al. 2005). The influence of natural (sisal, flax and cellulose) and synthetic (polypropylene, polyvinyl, and carbon) fibres on plastic shrinkage behaviour has been well researched (Banthia and Gupta 2006, Boghossian and Wegner 2008, Shah and Weiss 2006, Toledo et al. 2005). However, the mechanisms by which different fibres reduce plastic shrinkage strains and cracks have not been thoroughly studied. Further, studies with regards to the effect of basalt fibres on controlling plastic shrinkage are limited.

In the current study, a two-phase experimental program was undertaken. In phase I, the mechanical performance of three fibre types, namely bundled dispersion basalt fibres (BF), basalt minibars (MB), and commonly used hooked-end steel fibres (SF), were compared in terms of compressive, flexural, and impact strength. In phase II, the influence of basalt filament dispersion fibres (FD) on reducing free plastic shrinkage strain was assessed.

2   Experimental Program

2.1   Materials

Potable water and general use limestone (GUL) cement conforming to Canadian standard CSA A3001 (CSA 2013) were used in all mixtures. Fine aggregates (sand) and commercially available coarse aggregates (gravel) with a maximum size of 5 mm and 19 mm, respectively, were used. These particle sizes conformed to ASTM C33 (ASTM 2016). The fineness modulus and specific gravity of the sand were 2.63 and 2.51, respectively, whereas the specific gravity of the coarse aggregates was 2.55. A high range water-reducing admixture Type A&F, as recommended in ASTM C494 (ASTM 2016), was utilized for some mixtures to achieve the desired workability.

The fibres used in phase I were bundled dispersion fibres (BF), minibars (MB), and hooked-end steel fibres (SF), as shown in Figure 1. The BF used were either 36 mm or 50 mm long and 0.60 mm wide. These fibres were characteristically flat and consisted of 16 μm diameter filaments. On the other hand, the MB used were coated with epoxy-based resin and were 43 mm long with 0.65 mm diameter. The MB consisted of 17 μm diameter basalt filaments. The length and diameter of SF was 38 mm and 0.9 mm, respectively. For phase II, filament dispersion fibres (FD) of 25 mm length were used. FD had a similar width and filament diameter as BF.

(a) BF   (b) MB   (c) SF

Figure 1: Fibre types used in the concrete mixtures (Branston et al. 2016b)

2.2 Mixture Proportioning

The mixtures used in this study were different at each phase, as shown in Table 1. For phase I, concrete mixtures were proportioned having a water-cement ratio of 0.5 and proportions of 1:1.4:2.8 by mass of cement, fine aggregate, and coarse aggregate. The control mixture did not contain any fibres while the remaining mixtures were reinforced with either basalt (BF or MB) or steel (SF) fibres. Three levels of fibre amount were examined for each type of basalt fibre. When the maximum fibre content was used (12 kg/m^3 for BF and 40 kg/m^3 for MB), the workability of the mixtures was reduced, even with the addition of superplasticizer. The mixture names were designated to reflect the fibre type, fibre length, and fibre content. For example, mixture MB 43-20 refers to a concrete mixture that contains basalt minibars of 43 mm length and fibre content of 20 kg/m^3. For phase II, the concrete mixture proportions were 1:2:2 by mass of cement, fine aggregate, and coarse aggregate. The water-cement ratio used was 0.5. Similar to phase I, three levels of FD amount (1.3, 2.6, and 7.8 kg/m^3) were examined.

Table 1: Test matrix

Phase	Mixture Designation	Fibre length (mm)	Fibre Content kg/m^3	Fibre Content %	Fibre type
Phase I	Control	N/A	0	0	No fibre
	BF 36-4	36	4	0.15	Bundle dispersion
	BF 36-8		8	0.31	
	BF 36-12		12	0.46	
	BF 50-4	50	4	0.15	
	BF 50-8		8	0.31	
	BF 50-12		12	0.46	
	MB 43-6	43	6	0.31	Minibar
	MB 43-20		20	1	
	MB 43-40		40	2	
	SF 38-40	38	40	0.51	Steel fibre
Phase II	Control	N/A	0	0	No fibre
	FD 25-1.3	25	1.3	0.05	Filament dispersion
	FD 25-2.6	25	2.6	0.1	
	FD 25-7.8	25	7.8	0.3	

2.3 Test Methods

The compressive strength of phase I mixtures was conducted as per ASTM C39 (ASTM 2006). Upon casting and curing in lime-water, the specimens were air dried for two days until testing. The average 28-day strength of five capped cylinders were reported.

ASTM C1609 (ASTM 2006) was followed to test for third-point flexural strength, as shown in Figure 2. Beam specimens with a length of 610 mm and a cross-section of 152 mm by 152 mm were cast and tested. The deflection at the mid-span of the beams was measured using a 25 mm linear variable differential transformer (LVDT). The mean values reported for each mixture are based on three specimens tested after 28 days of curing.

The modified drop-weight impact test, specified by ACI Committee 544, was followed to evaluate the impact resistance of the phase I mixtures at 28 days. This method was recommended by Badr and Ashour (2005). Concrete specimens were cast in cylinder molds of 152 mm diameter by 305 mm height and triangular wood pieces of 25.4 mm dimensions were attached to each side to form notches. The notched cylinders were cut to specimens of 51 mm thickness. The impact resistance apparatus consisted of a 4.54 kg compaction hammer with a maximum drop height of 457 mm. For each specimen, the number of blows to initiate a visible surface crack and consequent failure was recorded. Specimens that exhibited cracking through a line between the notches were considered in the calculations and an average of 24 specimens were reported for each mixture. The test setup used (Figure 3) was similar to that of Branston et al. (2016b).

An environmental chamber capable of maintaining a required temperature of 45℃ (±2℃) and relative humidity of 15% (±2%) was used for testing free plastic shrinkage. The controller attached to the chamber measured the temperature and relative humidity with an accuracy of ±1.5℃ and ±2%, respectively. The resulting evaporation rate of the set conditions was approximately 1 kg/m^2/h. Figure 4 shows a schematic of the environmental chamber used.

Free plastic shrinkage testing was conducted using a method previously adopted by other researchers (Branston et al 2016a, Banthia and Gupta 2006), with several modifications to the dimensions of the test specimen. Mortar and concrete mixtures were cast in wooden molds with a length of 500 mm and cross-sectional area of 80 mm x 50 mm. A thick polypropylene sheet was placed on the inner surface of the molds and a thin layer of Teflon spray was applied on the sheet to minimize friction. A Teflon plate with a 9.5 mm diameter bolt was placed at one end of the mold. Upon placement of the concrete, the bolt was bonded with the test specimen and when shrinkage occurred, the plate moved linearly towards the direction of contraction. For each test specimen, a linear variable differential transformer (LVDT) was utilized to measure the linear movement of the Teflon plate. The LVDT had an accuracy of ± 5 µm. A 20 mm thick foam was also placed behind the Teflon plate to accommodate thermal expansion. Immediately after casting, the fresh concrete specimens were placed in the environmental testing chamber for four hours. The test setup for free shrinkage testing is illustrated in Figure 5.
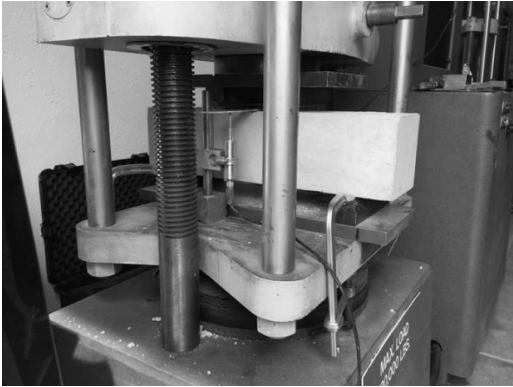
Figure 2: Flexural test setup (Branston et al. 2016b)   Figure 3: Impact test setup (Branston et al. 2016b)
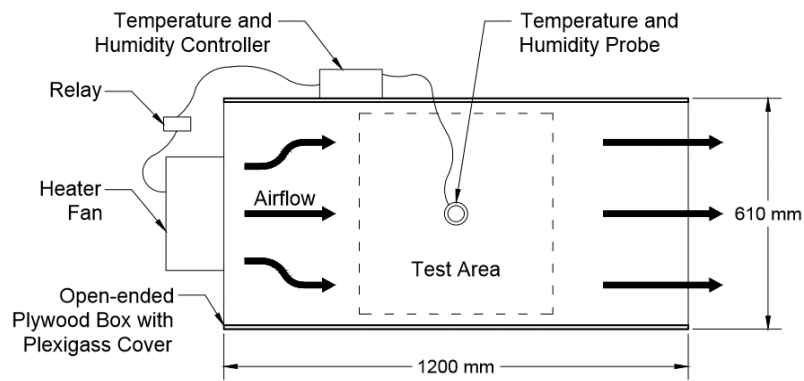

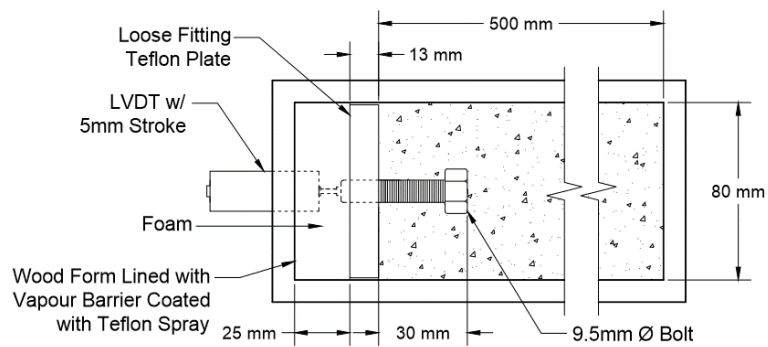Figure 4: Environmental chamber for free plastic shrinkage testing (Branston et al. 2016a)

Figure 5: Free plastic shrinkage test specimen setup (Branston et al. 2016a)

3 Results and Discussion

3.1 Compressive Strength Test

Compressive strength test was undertaken at the age of 28 days. The variation in compressive strength for each mixture is shown in Table 2. In general, it was found that mixtures containing BF exhibited compressive strengths slightly higher than the control and SF 38-40. However, a significant drop in strength was observed for mixtures containing MB. Nonetheless, it was observed during testing that specimens containing MB improved the toughness of the concrete under compression.

Table 2: Variation in compressive strength

Mixture Designation	Compressive Strength (MPa)
Control	37.7 (1.4)
BF 36-4	34.3 (1.2)
BF 36-8	39.2 (1.3)
BF 36-12	37.4 (2.0)
BF 50-4	38.2 (1.7)
BF 50-8	38.6 (2.3)
BF 50-12	38.7 (2.2)
MB 43-6	23.5 (1.6)
MB 43-20	20.7 (1.5)
MB 43-40	24.5 (1.6)
SF 38-40	35.6 (1.1)

Note: Values between parentheses represent the standard deviation of the mean

3.2 Flexural Test

Table 3 presents the results from the flexural tests. This table provides the obtained mid-span deflection (d_p); ultimate stress (f_p); residual strength at the mid-span deflection of L/600, where L denotes the span length ($f_L/600$); residual strength at the deflection of L/150 ($f_L/150$); and flexural strength ratio ($R_L/150$) calculated as per ASTM 1609 (2006). Based on the results obtained, the addition of BF in the concrete mixtures resulted in a slightly higher ultimate stress compared to the plain concrete (control). This is due to the fact that BF improves the strength and modulus of elasticity of concrete. The flexural stress also increases with the length of the fibre. Hence, BF mixtures with 50 mm fibres had a greater flexural stress compared to BF mixtures with 36 mm fibres. On the other hand, specimens containing MB were also effective in increasing the ultimate stress. Specimens reinforced with MB were more ductile after cracking and were capable of carrying between 55% and 85% of the peak-load at a deflection of 3 mm (L/150). This behaviour is likely due to the fibre pull-out failure mode experienced by the MB fibres. Further, the SF 38-40 specimen provided a similar increase in flexural stress as the MB 43-20 specimen and had comparable post-cracking behaviour as the MB 43-6 specimen.

Table 3. Flexural test results

Mixture Designation	d_p (mm)	f_p (MPa)	$f_L/600$ (MPa)	$f_L/150$ (MPa)	$R_L/150$ (%)
Control	0.33	4.01 (0.4)	0.17		
BF 36-4	0.36	4.38 (0.3)	1.17		
BF 36-8	0.22	4.71 (0.4)	0.14		
BF 36-12	0.31	4.94 (0.5)	0.41		
BF 50-4	0.29	4.42 (0.1)			
BF 50-8	0.28	4.85 (0.2)			
BF 50-12	0.28	5.10 (0.1)	0.33		
MB 43-6	0.17	4.01 (0.3)	2.14	2.13	54.35
MB 43-20	1.30	6.14 (0.5)	4.95	5.67	92.79
MB 43-40	2.00	9.22 (1.0)	7.51	8.69	93.71
SF 38-40	0.60	5.28 (0.4)	3.31	1.69	32.77

Note: Values between parentheses represent the standard deviation of the mean

3.3 Impact Test

Preliminary impact tests at a full drop height of 457 mm caused all plain concrete specimens to crack after a single blow, which resulted in the failure of the specimens after the second blow. Therefore, the drop-height was reduced to 152 mm in subsequent impact tests. For mixtures containing MB and SF, the specimens required more than 100 blows to fail. Accordingly, the full hammer drop height of 457 mm was used for these specimens after the first crack was observed. The results were then compared with the control specimen subjected to the same level of impact. The number of blows until first crack (N1) and the following number of blows until failure (N2) are presented in Table 4. Mixtures containing BF did not have a significant effect on the N1 and N2. However, increasing the MB content increased N2 by 1200% to 3000%. Specimens SF 38-40 and MB 43-20 exhibited comparable post-cracking impact strength (N2). Further, test observations of fractured MB specimens indicated that fibre pull-out governed the failure. However, fractured SF specimens exhibited fibre rupture as the governing source of failure. This behaviour is likely attributed to the hooked-ends of the SF fibres, which enhanced the bonding of the fibres to the cementitious matrix.

Table 4: Impact test results

Mixture Designation	Drop from 457 mm height		Drop from 152 mm height	
	N1	N2	N1	N2
Control		1.0	5.0	3.4
BF 36-4			3.7	2.3
BF 36-8			4.0	3.2
BF 36-12			4.2	2.3
BF 50-4			4.7	3.9
BF 50-8			5.6	4.4
BF 50-12			4.3	3.2
MB 43-6		13.3	5.3	
MB 43-20		19.4	8.2	
MB 43-40		30.6	9.4	
SF 38-40		19.7	6.5	

3.4   Free Plastic Shrinkage Test

The free plastic shrinkage results (Table 5) were based on the average of three test specimens. At FD contents of 1.3 kg/m^3 and 2.6 kg/m^3 (FD 25-1.3 and FD 25-2.6), it was found that shrinkage strains were slightly lower than that of plain concrete (control). However, increasing the fibre content to 7.8 kg/m^3 resulted in a 43% drop in shrinkage strain when compared with the control. This is due to the frictional force induced in the fibre-cement interface, which restrains the movement of cement (Mangat and Azari 1990).

Table 5: Mean plastic shrinkage strain values measured after four hours

Mixture Designation	Strain
Control	1610 x10^{-6}
FD 25-1.3	1596 x10^{-6}
FD 25-2.6	1597 x10^{-6}
FD 25-7.8	920 x10^{-6}

4   Conclusions

Based on the experimental results presented in this paper the following conclusions are drawn:

1. Mixtures containing BF generally resulted in higher compressive strength compared to the control. However, adding MB into the concrete resulted in a significant drop in compressive strength.
2. Overall, the addition of fibres improved the flexural properties of concrete. Increasing the amount and length of BF resulted in higher flexural stress. Similar findings were observed for concretes containing MB.
3. The impact test results for BF mixtures indicated that these fibres are not effective in improving impact loading. Nonetheless, concretes containing MB significantly improved post-cracking impact strength (N2) and SF 38-40 and MB 43-20 exhibited comparable behaviours.
4. Incorporating FD into concrete reduced strains associated with free plastic shrinkage. The reduction in strain can be attributed to the higher frictional force actuated at the fibre-cement interface which prevents the movement of the cement matrix.

References

ACI Committee 544. 544.1R-96: Report on Fibre Reinforced Concrete (Reapproved 2009). Technical Documents. 1996.

Adhikari, S. 2013. Mechanical and structural characterization of mini-bar reinforced concrete beams. Ph.D dissertation: The University of Akron.

ASTM C1609. 2006. Standard Test Method for Flexural Performance of Fibre Reinforced Concrete (using Beam with third-point loading. *Annual Book of ASTM Standards*, West Conshohocken Pennsylvania, PA.

ASTM C33. 2016. Standard specification for concrete aggregates. *Annual Book of ASTM Standards*, West Conshocken, PA.

ASTM C39. 2006. Standard Test Method for Compressive Strength of Cylindrical Concrete Specimens. *Annual Book of ASTM Standards*, West Conshohocken Pennsylvania; 2006.

ASTM C494. 2016. Standard specification for chemical admixtures for concrete. *Annual Book of ASTM Standards*, West Conshocken, PA.

Ayub, T., Shafiq, N., Nuruddin, MF. 2014. Mechanical Properties of High-Performance Concrete Reinforced with Basalt Fibres. *Procedia Engineering* 77:131-9.

Badr, A and Ashour, AF. 2005. Modified ACI drop-weight impact test for concrete. *ACI Materials Journal* 102(4):249-55.

Banthia, N. and Gupta, R. 2006. Influence of polypropylene fibre geometry on plastic shrinkage cracking in concrete. *Cement and Concrete Research* 36(7):1263-7.

Boghossian, E. and Wegner, LD. 2008. Use of flax fibres to reduce plastic shrinkage cracking in concrete. *Cement and Concrete Composites* 30(10):929-37.

Borhan TM. Thermal and mechanical properties of basalt fibre reinforced concrete. Proceedings of World Academy of Science, Engineering and Technology: World Academy of Science, *Engineering and Technology* (WASET), 7:334-337.

Branston, J., Das, S., Kenno, S.Y., Taylor, C. 2016a. Influence of basalt fibres on free and restrained plastic shrinkage. *Cement and Concrete Composites* 74:182–90.

Branston, J., Das, S., Kenno, S., and Taylor, C. 2016b. Mechanical behaviour of basalt fibre reinforced concrete, *Construction and Building Materials* 124: 878-886.

CSA A3001. 2013. Cementitious materials used in concrete. *Canadian Standards Association*, Mississuiga, Ontario.

Dias DP., Thaumaturgo, C. 2005. Fracture toughness of geopolymeric concretes reinforced with basalt fibres. *Cement and concrete composites* 27(1):49-54.

Iyer, P., Kenno, SY., Das, S. 2015. Mechanical Properties of Fibre-Reinforced Concrete Made with Basalt Filament Fibres. *Journal of Materials in Civil Engineering, ASCE* 27(11):04015015.

Jiang, C., Fan, K, Wu, F, Chen, D. 2014. Experimental study on the mechanical properties and microstructure of chopped basalt fibre reinforced concrete. *Materials and Design* 58:187-93.

Naaman, AE., Wongtanakitcharoen, T., Hauser, G. 2005.Influence of different fibres on plastic shrinkage cracking of concrete. *ACI materials Journal* 102(1):49-58.

Shah, H., and Weiss, J. 2006. Quantifying shrinkage cracking in fibre reinforced concrete using the ring test. *Materials and structures* 39(9):887-99.

Soroushian P. and Ravanbakhsh S. 1998. Control of plastic shrinkage cracking with speciality cellulose fibres. *ACI Materials Journal* 95:429-435.

Toledo Filho RD., Ghavami, K., Sanjuán, MA., England, GL. 2005. Free, restrained and drying shrinkage of cement mortar composites reinforced with vegetable fibres. *Cement and Concrete Composites* 27(5):537-46.